

## Research Article

# Development of a Stable TiO<sub>2</sub> Nanocomposite Self-Cleaning Coating for Outdoor Applications

F. Madidi, G. Momen, and M. Farzaneh

Canada Research Chair on Atmospheric Icing Engineering of Power Networks (INGIVRE), Université du Québec à Chicoutimi, Chicoutimi, QC, Canada G7H 2B1

Correspondence should be addressed to F. Madidi; [fmadidi@gmail.com](mailto:fmadidi@gmail.com)

Received 22 February 2016; Accepted 22 May 2016

Academic Editor: Michael Aizenshtein

Copyright © 2016 F. Madidi et al. This is an open access article distributed under the Creative Commons Attribution License, which permits unrestricted use, distribution, and reproduction in any medium, provided the original work is properly cited.

A convenient and low-cost approach for the elaboration of a stable superhydrophobic coating is reported, involving the use of TiO<sub>2</sub> nanoparticles via the spray coating method. This method can be used for preparing self-cleaning superhydrophobic coatings on large areas for different kinds of substrates. The synergistic effect of the micro/nanobinary scale roughness was produced by a multilayer RTV SR/TiO<sub>2</sub> composite. The influence of the nanofiller concentration in a specific frequency range (40 Hz to 2 MHz) on the dielectric behavior was analyzed as well. It was found that the real relative permittivity ( $\epsilon_r'$ ) increases as the nanofiller concentration increases. Superhydrophobic behavior is analyzed by contact angle measurements, scanning electron microscopy (SEM), and profilometer. The stability of the developed coating also has been evaluated in terms of immersion in various aqueous solutions, heating, adhesion, and exposure to UV irradiation, and the results showed good stability against these factors. The coating retained its superhydrophobicity after several days of immersion in solutions of different pH levels (2, 4, 6, and 12) and different conductivities. In addition, they also exhibited exceptional stability against UV radiation and heating, as well as good mechanical stability.

## 1. Introduction

Pollution accumulation on structures is a serious and costly problem affecting a wide variety of human activities such as electric power transmission and distribution [1, 2].

One of the approaches to avoid these problems is to prevent the adhesion and accumulation of the contaminants on the surfaces through the development of superhydrophobic and self-cleaning coatings.

Superhydrophobic coatings have a static contact angle greater than 150° and a low contact angle hysteresis between 2° and 10°. These surfaces are commonly prepared in a two-step process: surface roughness creation and coating with a low surface energy material. The most popular methods to create superhydrophobic surfaces are sol-gel [3, 4], anodization [5], chemical etching [6], self-assembly [7], electrochemical deposition [8], electrospinning [9], plasma treatment [10], and others.

However, these techniques all require either special equipment or complex process control. Therefore, it would

be very beneficial and practical if superhydrophobic surfaces were obtained in just a one-step process using inexpensive materials and application method. The spray coating method using a nanocomposite can fulfill this demand because of its rapidity and simplicity of application to large surface areas.

For high voltage (HV) equipment, especially in outdoor environments, silicone rubber is considered to be the best in class elastomer due to its hydrophobicity. In order to improve properties of silicone rubber and to extend its service life, nanoparticles are added to the base polymer. The addition of these nanoparticles can increase the surface hydrophobicity, the relative permittivity, and the electrical conductivity of composite silicone. Thus, the surface constraints can be considerably reduced. RTV silicone rubber reinforced with semiconducting materials, such as TiO<sub>2</sub> nanoparticles, is expected to lead to improved electric field distribution on outdoor insulators [11]. Furthermore, the electrical stresses on reinforced insulators can be significantly reduced, since the introduction of inorganic fillers can enhance the homogeneity and distribution of the electric field on their surface [12].

A major challenge in this field is to develop a practical and industrially feasible method to prepare superhydrophobic coatings with good stability against adverse environmental influences. In addition, the stability of superhydrophobic coatings is evaluated by changes of water contact angle and contact angle hysteresis, which indicates that water drops are sticky on the surface after mechanical or chemical damage. The adhesion of water drops on a surface means a loss of the self-cleaning property. Concerning the stability of superhydrophobic coatings, not much research has been done [13, 14]. Feng et al. [13] report superhydrophobic nanostructured carbon films that maintain static contact angles above  $150^\circ$  after 24 h immersion in pure water (pH 7), acidic solution (pH 1), and basic solution (pH 14). Yan et al. [14] report unaltered static contact angles after immersion of super water repellent poly(alkylpyrrole) films in solvents, in hot and cold water, without providing immersion times.

The present study is expanded to include several environmental factors such as immersion in different solutions, UV radiation, heating, and mechanical stability.

Also, the dielectric behavior of RTV silicone rubber reinforced with different  $\text{TiO}_2$  concentrations was investigated. The  $\text{TiO}_2$  nanoparticles were modified by Triton X-100, a common surfactant, to improve the uniformity of nanofiller dispersion. The surfactant enhances the separation of the particles and improves their dispersion during mixing.

The RTV SR/ $\text{TiO}_2$  composite was also characterized by means of scanning electron microscopy (SEM), profilometer, and impedance analyzer.

## 2. Materials and Methods

Commercial RTV silicone rubber containing 40–70 wt% alumina hydrate and titanium dioxide ( $\text{TiO}_2$ ) nanoparticles with an average size  $<25$  nm obtained from Sigma Aldrich were used in the present study. Glass substrates were cleaned in acetone and water.

Initially,  $\text{TiO}_2$  particles were dried at  $100^\circ\text{C}$  for 24 hours before mixing with silicone rubber. The dispersion of nanoparticles was the most difficult step since it determined the final properties of the nanocomposite.

A specific amount of filler particles (based on weight fractions) was mixed with isopropanol. Subsequently, the as-prepared solution was placed in an ultrasonic bath for 20 minutes; then it was mechanically stirred at 700 RPM for 2 hours in order to ensure a good dispersion of nanoparticles and a homogenized solution. RTV SR was added to the previously described solution. This solution was then placed into the ultrasonic bath for 60 minutes and then mechanically stirred at 600 RPM for of 2 hours.

The solutions were coated on clean dry glass slides with nitrogen gas by means of a spray gun. Heat treatment of the coatings was done at  $80^\circ\text{C}$  in air overnight to remove residual solvents.

For this study, RTV SR/ $\text{TiO}_2$  samples were prepared. We opted for multilayer deposition coatings. Also, we were able to optimize the number of deposits to three layers, since some superhydrophobicity was lost by adding a fourth layer; this may be due to the loss of roughness.

Nanoparticles are highly charged materials which tend to agglomerate and form larger particles. This agglomeration process significantly reduces the nanoparticle surface to a volume ratio which in turn compromises the unique nanoparticle properties in the polymer [15]. Therefore, a commercial surfactant, Triton X-100, was used to disperse the nanofillers.

For experiments on dielectric properties, nanocomposites were prepared using a combination of two different processing techniques: mechanical mixing and ultrasonication. A specific amount of filler particles (based on weight fractions) was mixed with a solvent and  $0.3\ \mu\text{L}$  of a nonionic Triton X-100. Subsequently, the as-prepared solution was placed in an ultrasonic bath for 20 minutes and then mechanically stirred at 700 RPM for a period of 2 hours. Then, RTV SR was added to the solution previously described. This solution was then placed back into the ultrasonic bath for 60 minutes and then mechanically stirred at 600 RPM for a period of 24 hours.

For this study, six RTV SR/ $\text{TiO}_2$  samples with 0, 2, 5, 10, and 20 wt%  $\text{TiO}_2$  were prepared.

The wettability of these coatings was investigated using distilled water and a DSA-100 contact angle (CA) measuring instrument from Krüss. The morphological characterization was examined using a LEO scanning electron microscope (SEM) and the surface roughness was measured using a confocal profilometer CHR 150-L.

The dielectric permittivity was measured using an Agilent 4294A impedance analyzer over the frequency range of 40 Hz–2 MHz.

## 3. Results and Discussions

**3.1. Superhydrophobic Properties.** In order to improve the stability of superhydrophobic coatings, we opted for a multilayer coating. The number of layers was optimized to three since superhydrophobicity was lost for more than three multilayers.

**3.1.1. Morphology of Monolayer and Multilayer Coatings.** Roughness is a key parameter that affects the wettability of a surface [16]. The variation in the morphological characteristics of the surface is shown in Figure 1. The value of roughness is in root mean square (Rq).

Figure 1(a) shows the morphology of a SR/ $\text{TiO}_2$  coating with a single superhydrophobic layer. The thickness of the as-prepared coating is  $4\ \mu\text{m}$ . Figure 1(b) shows the same coating with three superhydrophobic layers, the thickness of this coating being  $25\ \mu\text{m}$ . Figures 1(a) and 1(b) show a surface state for the least roughness in the case of the monolayer coating and a maximum roughness in the case of the multilayer coating. Quantitative analysis based on these images indicates that the average roughness (Rq) is  $1.88\ \mu\text{m}$  for Sample (a), which is composed of a single layer, while it increases to  $11.6\ \mu\text{m}$  for Sample (b), composed of three layers.

**3.1.2. Effect of Number of Layers on Stability of Superhydrophobic Coatings in an Acid Solution.** The durability of superhydrophobic coatings is an important factor to be

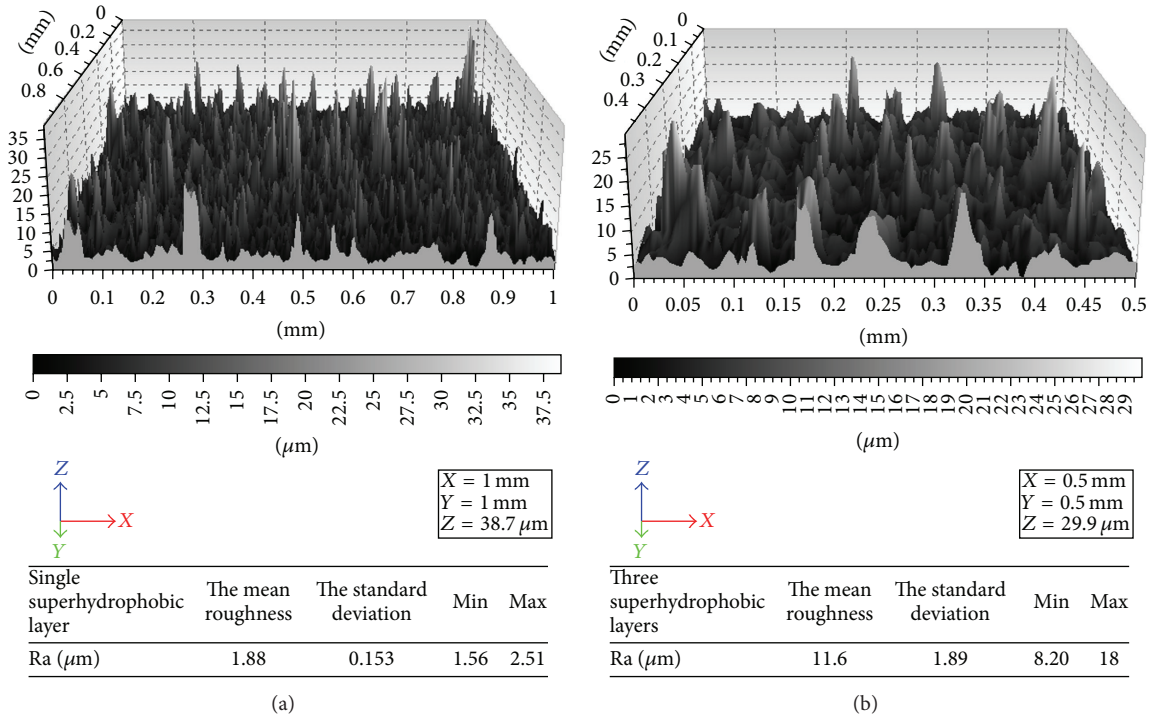


FIGURE 1: Images of the 3D topographic surface obtained by profilometry for (a) a single superhydrophobic layer and (b) three superhydrophobic layers.

investigated. The lifetime of a coating depends largely on coating/substrate adhesion.

Figures 2(a) and 2(b) show a coating with a single superhydrophobic layer ( $4 \mu\text{m}$ ) after 40 days of immersion in an acid solution ( $\text{pH} = 5$ ). One can clearly see that the polymeric filaments are completely removed by the acid. Figures 2(c) and 2(d) show a coating with three superhydrophobic layers ( $25 \mu\text{m}$ ) after 40 days of immersion in the same solution. This coating reveals a continuous recovery of the surface by the polymer. A significant presence of agglomeration and roughness is also observed which is responsible for superhydrophobicity.

SEM analysis shows that the sample obtained with three superhydrophobic layers is less affected by the acid compared to the sample prepared by a single layer.

**3.1.3. Stability of Superhydrophobic Coatings in Different Solutions.** In order to study the stability of as-prepared superhydrophobic coatings in different environmental conditions, their stability was studied in different pH solutions ( $\text{pH} 2, 4,$  and  $12$ ). These values were chosen considering some of the common contaminants and environments: washing solution has a pH value ranging from 9 to 12 [17], acid rain has a pH value of about 4 [18], and the tap water has a pH value of 6. Solutions with different conductivities ( $30 \mu\text{s}\cdot\text{m}^{-1}$ ,  $60 \mu\text{s}\cdot\text{m}^{-1}$ , and  $100 \mu\text{s}\cdot\text{m}^{-1}$ ) were also tested which may represent polluted rain.

Momen and Farzaneh [18] have proposed the spray coating approach for the development of superhydrophobic coatings. After obtaining such coatings, they studied their

stability. They showed that the incorporation of 1g of ZnO nanoparticles increases static contact angle from  $117^\circ$  to  $132.5 \pm 2^\circ$ . After the incorporation of a small amount of  $\text{SiO}_2$  (10 nm), a significant increase in the contact angle was observed ( $162^\circ$ ).

To assess the stability of the superhydrophobic coating RTV-ZnO-SiO<sub>2</sub>, coating samples were immersed in solutions of different pH values. The results showed a slight decrease in the contact angle for the samples immersed in buffer solutions of pH after 10 days. However, all samples maintained their superhydrophobicity. The contact angle hysteresis was more affected by immersion in pH buffers, as the values of contact angle hysteresis were significantly increased and the samples almost lost their roll-off behavior after two days. Guo et al. [19] have developed thin superhydrophobic polyaniline (PANI) coatings by polymerization of aniline. These coatings have a high contact angle and low contact angle hysteresis. After several hours of immersion in water and in acidic solutions, these coatings maintained their superhydrophobicity. Wang et al. [20] have obtained superhydrophobic coatings which retained their properties after five days of immersion in acetone, ethanol, and toluene.

In the present paper, the results of a study on the stability of a SR/TiO<sub>2</sub> with 10 wt% TiO<sub>2</sub> multilayer coating are presented. Aqueous resistance at different pH values and conductivities was evaluated in terms of contact angle and contact angle hysteresis.

Figure 3 shows the variation of the static contact angle as a function of immersion time in the above mentioned solutions.

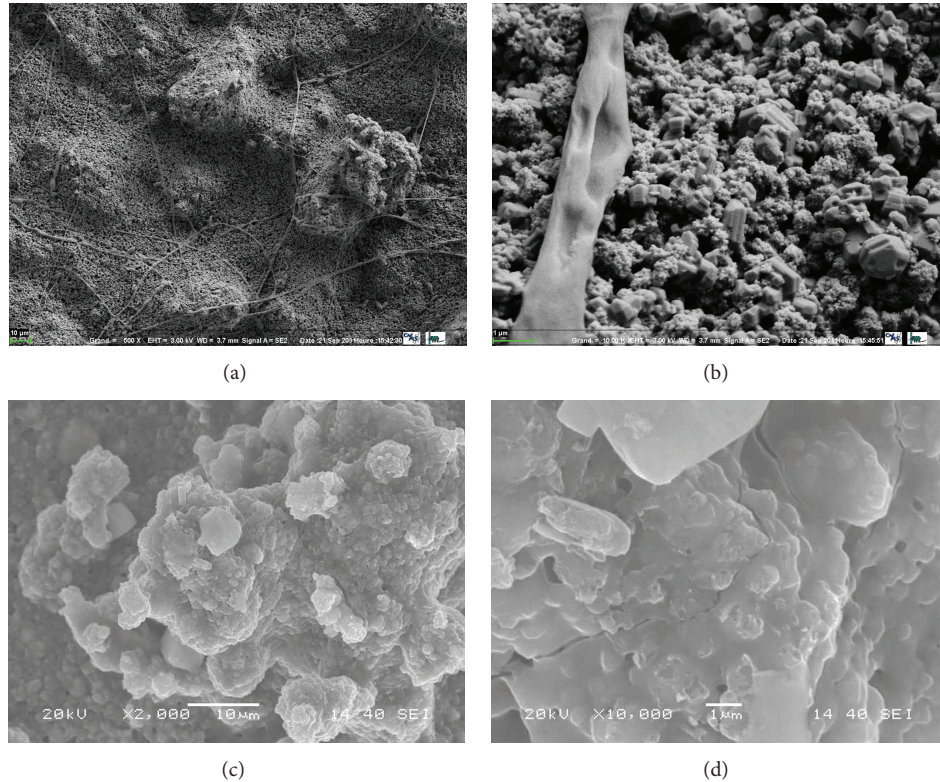


FIGURE 2: Effect of the number of layers on the stability of superhydrophobic coatings. (a, b) A single layer; (c, d) three layers.

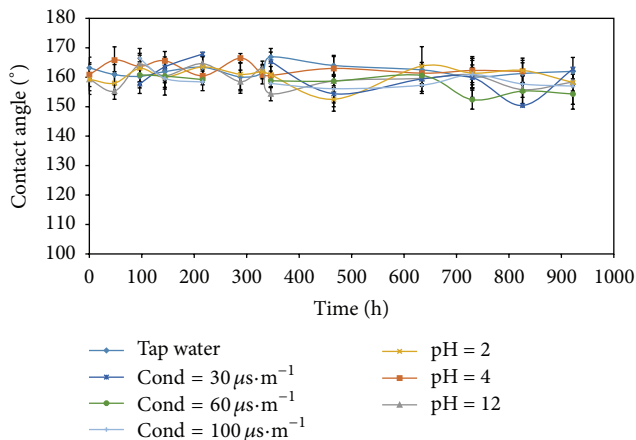


FIGURE 3: Variation in the static contact angle as a function of immersion time in different solutions.

The results in Figure 3 have shown a marked decrease in the contact angle for the sample immersed in the solution at  $30 \mu\text{s}\cdot\text{m}^{-1}$  after 800 hours of immersion. This decrease is due to the ionic contamination and localized deposition of NaCl molecules. The deposition of NaCl particles on the coating was verified by SEM and EDX analysis (Figure 4). However, all samples immersed in the solutions above had maintained their superhydrophobicity after 922 hours.

TABLE 1: Contact angle hysteresis of the prepared coatings.

Time (h)	Tw (CAH)	pH = 2 (CAH)	pH = 4 (CAH)	pH = 12 (CAH)
0	1	3	1.1	2
922	2	3.7	12.7	9.3

The variations of contact angle hysteresis of the superhydrophobic coating after a 922 h immersion in different pH solution are listed in Table 1.

It was observed that contact angle hysteresis increases after 922 hours of continuous immersion in solutions at pH = 4 and pH = 12. This could be attributed to a slight loss of roughness or to a low degradation of the coating. However, the samples did not lose their “roll-off” properties.

**3.1.4. UV and Humidity Stability.** Sunlight is a major cause of damage for many kinds of materials, including plastics, textile, coatings, and other organic materials. The type of damage, such as loss of physical properties, chalking, cracking, peeling, fading, and color change, varies depending on material sensitivity and spectrum of sunlight [21].

In order to simulate sunlight exposure, the sample was exposed to a UVA fluorescent lamp. The contact angle was measured after several hours of exposure.

In order to assess the stability of the hydrophobic properties of the multilayered SR/TiO<sub>2</sub> coating under UV irradiation, accelerated aging tests were conducted according to

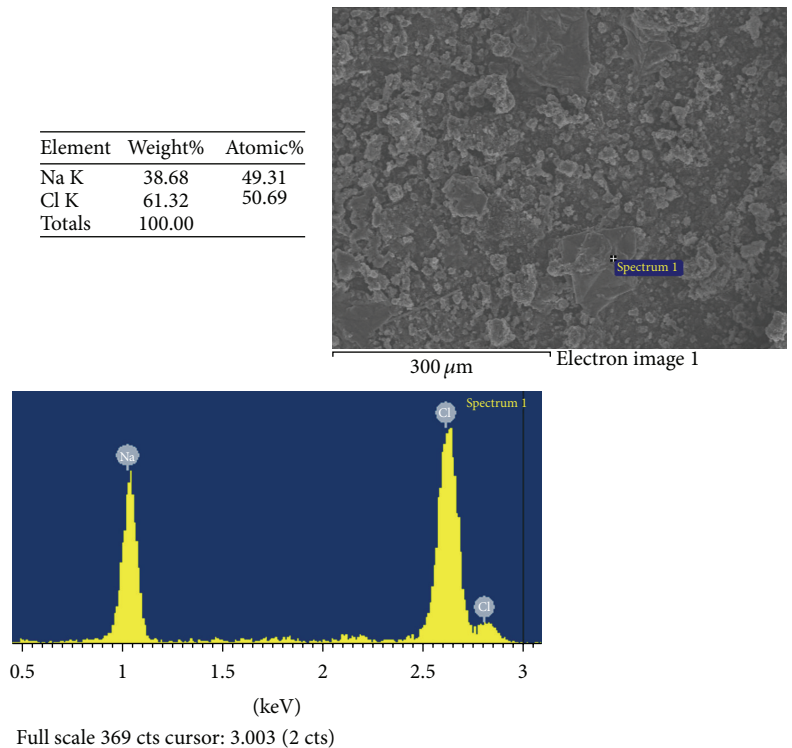


FIGURE 4: Analysis of the chemical composition of the sample immersed in the solution of 1-conductivity 30  $\mu\text{s}\cdot\text{m}$ .

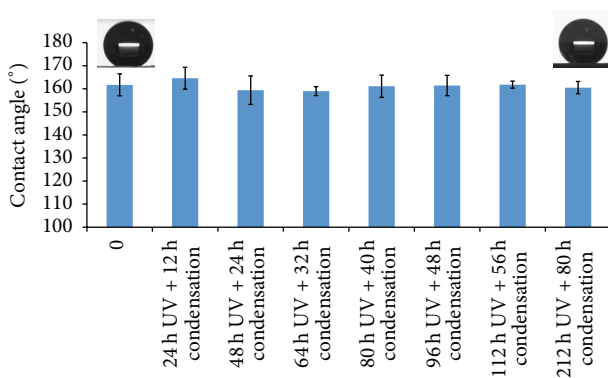


FIGURE 5: UV stability test results for the superhydrophobic coating.

the ASTM G154 standard. Indeed, every test performed by the QUV-accelerated device includes UV exposure and condensation. Superhydrophobicity of the surfaces is retained even after 212 hours of UV exposure and 80 hours of condensation, as shown in Figure 5. No significant effect and no color change were observed after UV and humidity cycle exposures.

**3.1.5. Stability against Heating.** Hydrophobic thermal stability is a very important physical property of coating materials from the point of view of applications. Thermal deterioration and thermal instability of materials can exert a negative influence on superhydrophobic coatings exposed to high temperature. Therefore, thermal stability of a coating is also an important property which was investigated by heating

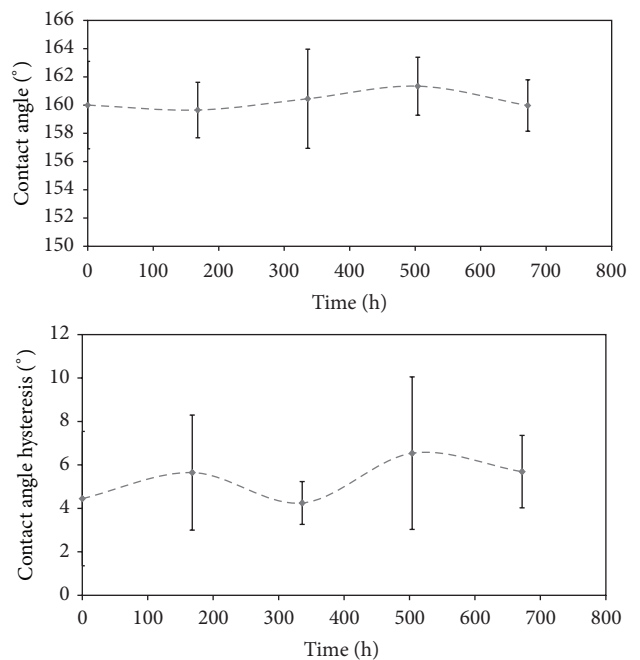


FIGURE 6: Thermal stability of the prepared superhydrophobic surface versus time.

the SR/TiO<sub>2</sub> sample at temperatures up to 150°C for different periods of time. The superhydrophobic coating exhibited excellent stability following the heat treatment, as shown in Figure 6. A high static contact angle of 160° and low contact

angle hysteresis  $\leq 6^\circ$  were obtained for the sample placed in the oven for almost a month. So, the prepared nanocomposite coating pretty much retained its superhydrophobic and roll-off properties after the heat treatment.

**3.1.6. Adhesion and Mechanical Properties of the Coating.** Adhesion force between a substrate and a coating is affected by several physical and chemical phenomena at the interface. It mainly depends on the bonds existing at the interfacial zone, where mechanical stress can lead to adhesion failure. Interfacial interactions can be categorized into three groups [22].

**Mechanical Anchorage.** In this type of interaction, adhesion originates from macroscopic interlocking between the two materials in contact, in particular for the anchoring of the coating to asperities on the surface of the substrate.

**Interatomic or Intermolecular Bonds.** Interaction between the electrons on the surface can give rise to interatomic forces, such as covalent, ionic, or metallic bonds. Intermolecular bonds, on the other hand, are forces present between two molecules, such as Van Der Waals or hydrogen forces. These intermolecular bonds are generally weaker than interatomic forces [23].

**Interdiffusion.** In the case of polymeric materials, the diffusion of long chain molecules can lead to a cross-linked network which can improve the adhesion force. This phenomenon leads to the formation of an interphase whose properties vary depending on the structure and compatibility of the polymers used in contact.

The adhesion properties of a system are generally evaluated using mechanical tests. In this study, a uniaxial adhesion test is used to apply a force normal to the substrate surface and measure the force at the failure point.

Table 2 shows the results of peel force for three samples: two superhydrophobic samples (one covered with a single layer and the other one with three layers) and one painted control sample.

This adhesion test was carried out according to ISO 4624 or ASTM D4541 and can determine the adhesion of a coating relatively easily.

The results provide a quantitative value of the bond (expressed in MPa, kg/m, N/mm<sup>2</sup>, PSI...). It is a suitable test procedure to compare different coating systems when it comes to their adhesive properties.

The adhesion stress for the three-layer coating was determined to be 0.87 MPa, while the one-layer coating had an adhesion stress of 0.59 MPa. The adhesion stress of metallic paint on aluminum is in the same range as the three-layer coating, which may suggest that the three-layer coating can meet the mechanical adhesion requirements in the industry.

**3.2. Dielectric Properties.** After developing stable superhydrophobic coatings, the evolution of the dielectric properties of nanocomposite coatings was examined for silicone rubber with different concentrations of TiO<sub>2</sub>.

TABLE 2: Peel force for two different samples SR/TiO<sub>2</sub>.

Number of superhydrophobic layers	Flexural strength (MPa)
One superhydrophobic layer	0.59 MPa
Three superhydrophobic layers	0.87 MPa
Paint on aluminum	0.96 MPa

**3.2.1. Morphology Characterization.** The structural morphology of the fabricated nanocomposites was observed for SEM. RTV SR/TiO<sub>2</sub> samples containing 5% titanium dioxide by weight, with and without the addition of surfactant, were prepared to investigate the effects of the surfactant on the dispersion of the nanoparticles in the polymer matrix (Figure 7).

Triton X-100 (C<sub>14</sub>H<sub>22</sub>O(C<sub>2</sub>H<sub>4</sub>O)<sub>n</sub> where n = 9-10) was used as surfactant. Triton X-100 was already used by Ramirez et al. to achieve a better dispersion of the nanofiller [24]. They compared the degree of dispersion of the nanofillers for the samples containing 5% nanosilica by weight, with and without added surfactant. The results showed that Triton X greatly improves the dispersion of nanosized particles, yielding nanocomposites that are more homogeneous [24].

It was observed that the surface morphology of the sample with the surfactant (a) is very different from that of the sample without the surfactant (b).

In Figure 7(a), the nanoparticles are dispersed uniformly in the polymer matrix, clearly showing that the introduction of Triton X leads to a significant reduction in the number of agglomerates by reducing the surface energy and therefore separating the agglomerates, which subsequently improves the dispersion of the nanoparticles.

**3.2.2. Effect of Filler Concentration on the Real Part of Relative Permittivity.** Dielectric materials like silicone rubber possess relatively few free charge carriers, which prevents the circulation of a significant electric current. However, the charges present in the matrix can be displaced under the effect of an external electric field and generate a current. This current is due to the polarization of the dielectric which may involve the following types of mechanism:

- (i) electronic;
- (ii) ionic/atomic;
- (iii) rotation/orientation;
- (iv) interfacial polarization.

Polarization is measured in terms of permittivity.

Permittivity determines the load storage capacity of a dielectric material and its electric field strength:

$$\kappa^* = \epsilon_r^* = \frac{\epsilon^*}{\epsilon_0} = \epsilon_r' - j\epsilon_r'' \quad (1)$$

Equation (1) shows that the dielectric constant ( $\kappa$ ) is equivalent to the complex relative permittivity ( $\epsilon_r^*$ ) or the complex permittivity ( $\epsilon^*$ ) relative to the permittivity of free space ( $\epsilon_0$ ). The real part of complex relative permittivity ( $\epsilon_r'$ ) is a measure of how much energy from an external field is stored in

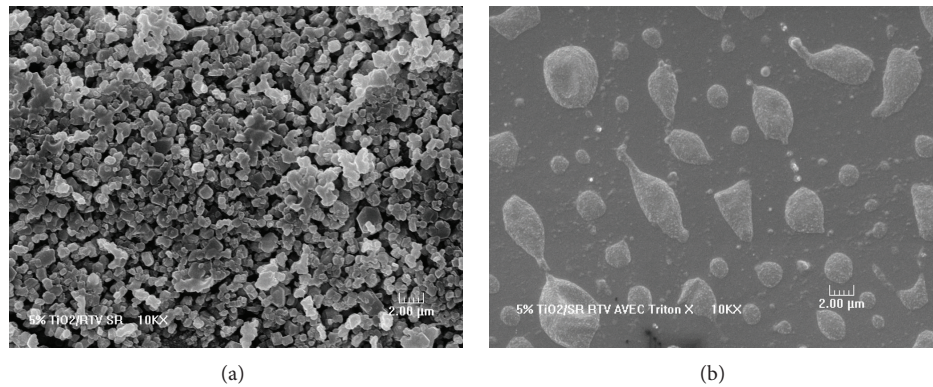


FIGURE 7: Effect of Triton X on the nanoparticles dispersion for RTV silicone rubber/ $\text{TiO}_2$  (5 wt%): (a) with surfactant; (b) without surfactant.

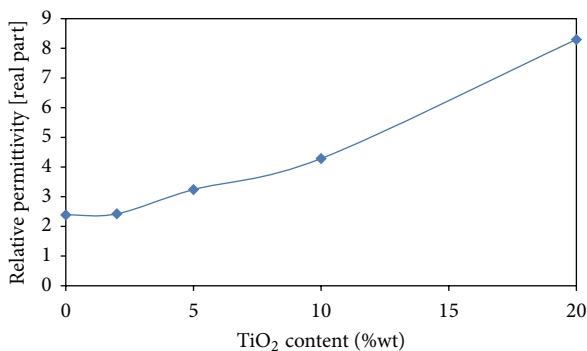


FIGURE 8: Effect of filler concentration on the real part of relative permittivity.

a material; the imaginary part of complex relative permittivity ( $\epsilon_r''$ ) is a measure of how dissipative or lossy a material is to an external field.

An Agilent 4294A impedance analyzer was used to measure the dielectric permittivity of the nanocomposite over the frequency range of 40 Hz–2 MHz. The variation of the real part of the permittivity for RTV silicone rubber reinforced with different concentrations of  $\text{TiO}_2$  nanofiller at 165 Hz is shown in Figure 8.

Permittivity of the nanocomposites is mainly governed by two factors: (1) the polarization associated with RTV silicone rubber and the  $\text{TiO}_2$  nanoparticles and (2) the interfacial polarization at the interface between the polymer and the nanoparticles.

Nanocomposite reinforced RTV silicone rubber tends to have a higher relative permittivity within a lower frequency range, which is attributed to interfacial polarization (IP) or to the Maxwell-Wagner-Sillars polarization.

Maxwell Wagner-Sillars polarization occurs in heterogeneous materials where polarization is the consequence of solid interface effects which strongly depend on microstructure and constituent materials.

It can be seen from Figure 8 that the real relative permittivity ( $\epsilon_r'$ ) increases as the  $\text{TiO}_2$  content in the RTV SR is increased. Since the individual permittivity of  $\text{TiO}_2$  is

higher than that of pure silicone rubber, it will influence the value of the resultant nanocomposite permittivity.

Also, it can be observed that, at a frequency of 165 Hz and 20 wt%  $\text{TiO}_2$  loading, the real part of permittivity is quadrupled. The addition of  $\text{TiO}_2$  with permittivity higher than that of the base polymer increases the permittivity of the polymer composite, mainly due to the influence of the filler permittivity.

It can also be shown that increasing the nanofiller concentration in RTV silicone rubber causes the permittivity to increase.

#### 4. Conclusion

In this study, a stable RTV silicone rubber/titanium dioxide nanocomposite was prepared using a convenient spray coating method. The number of deposited coatings was optimised to three layers, since some superhydrophobicity would be lost by adding a fourth layer.

The resulting superhydrophobic coating exhibited excellent stability following immersion in various aqueous solutions as well as exposure to UV irradiation, heating, and humidity. The coating retained its superhydrophobicity after being immersed 40 days in solutions of different pH and conductivity levels. The coating also exhibited good mechanical stability.

Moreover, the addition of  $\text{TiO}_2$  contributed to increase relative permittivity of the RTV silicone rubber. The highest relative permittivity in the nanocomposites with  $\text{TiO}_2$  was observed at the highest filler concentration of 20%. This suggests a promising area of study for outdoor insulation applications.

#### Competing Interests

The authors declare that they have no competing interests.

#### Acknowledgments

This work was carried out within the framework of the Canada Research Chair on Engineering of Power Network

Atmospheric Icing (INGIVRE) at Université du Québec à Chicoutimi. The authors would like to thank the INGIVRE partners (Hydro-Québec, Hydro One, Réseau de Transport d'Électricité (RTE), Alcan Cable, K-Line Insulators, Dual-ADE, and FUQAC) whose financial support made this research possible. The authors are grateful to Patrick Portes (LSPM-Paris-FRANCE) for SEM analysis. They would also like to thank Dr. Reza Jafari for his help and useful discussions.

## References

- [1] R. Boudissa, A. Bayadi, and R. Baersch, "Effect of pollution distribution class on insulators flashover under AC voltage," *Electric Power Systems Research*, vol. 104, pp. 176–182, 2013.
- [2] A.-S. H. A. Hamza, S. A. Mohmoud, and S. M. Ghania, "Environmental pollution by magnetic field associated with power transmission lines," *Energy Conversion and Management*, vol. 43, no. 17, pp. 2443–2452, 2002.
- [3] S. S. Latthe, H. Imai, V. Ganesan, and A. V. Rao, "Superhydrophobic silica films by Sol-Gel Co-precursor method," *Applied Surface Science*, vol. 256, no. 1, pp. 217–222, 2009.
- [4] V. V. Ganbavle, U. K. H. Bangi, S. S. Latthe, S. A. Mahadik, and A. V. Rao, "Self-cleaning silica coatings on glass by single step sol-gel route," *Surface and Coatings Technology*, vol. 205, no. 23–24, pp. 5338–5344, 2011.
- [5] S. He, M. Zheng, L. Yao et al., "Preparation and properties of ZnO nanostructures by electrochemical anodization method," *Applied Surface Science*, vol. 256, no. 8, pp. 2557–2562, 2010.
- [6] J. Ou, W. Hu, S. Liu, M. Xue, F. Wang, and W. Li, "Superoleophobic textured copper surfaces fabricated by chemical etching/oxidation and surface fluorination," *ACS Applied Materials and Interfaces*, vol. 5, no. 20, pp. 10035–10041, 2013.
- [7] Z. Duan, Z. Zhao, D. Luo, M. Zhao, and G. Zhao, "A facial approach combining photosensitive sol-gel with self-assembly method to fabricate superhydrophobic TiO<sub>2</sub> films with patterned surface structure," *Applied Surface Science*, vol. 360, pp. 1030–1035, 2016.
- [8] C.-T. Hsieh, S.-Y. Yang, and J.-Y. Lin, "Electrochemical deposition and superhydrophobic behavior of ZnO nanorod arrays," *Thin Solid Films*, vol. 518, no. 17, pp. 4884–4889, 2010.
- [9] U. Cengiz, M. Z. Avci, H. Y. Erbil, and A. S. Sarac, "Superhydrophobic terpolymer nanofibers containing perfluoroethyl alkyl methacrylate by electrospinning," *Applied Surface Science*, vol. 258, no. 15, pp. 5815–5821, 2012.
- [10] Y. Zhang, Y. Li, J. Shao, and C. Zou, "Fabrication of superhydrophobic fluorine-free films on cotton fabrics through plasma-induced grafting polymerization of 1,3,5,7-tetravinyl-1,3,5,7-tetramethylcyclotetrasiloxane," *Surface and Coatings Technology*, vol. 276, pp. 16–22, 2015.
- [11] G. Momen and M. Farzaneh, "Survey of micro/nano filler use to improve silicone rubber for outdoor insulators," *Reviews on Advanced Materials Science*, vol. 27, pp. 1–13, 2011.
- [12] E. A. Cherney, "Silicone rubber dielectrics modified by inorganic fillers for outdoor high voltage insulation applications," *IEEE Transactions on Dielectrics and Electrical Insulation*, vol. 12, no. 6, pp. 1108–1115, 2005.
- [13] L. Feng, Z. Yang, J. Zhai et al., "Superhydrophobicity of nanostructured carbon films in a wide range of pH values," *Angewandte Chemie*, vol. 42, no. 35, pp. 4217–4220, 2003.
- [14] H. Yan, K. Kurogi, H. Mayama, and K. Tsujii, "Environmentally stable super water-repellent poly(alkylpyrrole) films," *Angewandte Chemie—International Edition*, vol. 44, no. 22, pp. 3453–3456, 2005.
- [15] S. Singha and M. J. Thomas, "Permittivity and tan delta characteristics of epoxy nanocomposites in the frequency range of 1 MHz–1 GHz," *IEEE Transactions on Dielectrics and Electrical Insulation*, vol. 15, no. 1, pp. 2–11, 2008.
- [16] T. Ishizaki, N. Saito, Y. Inoue, M. Bekke, and O. Takai, "Fabrication and characterization of ultra-water-repellent alumina-silica composite films," *Journal of Physics D: Applied Physics*, vol. 40, no. 1, pp. 192–197, 2007.
- [17] J. Zimmermann, F. A. Reifler, G. Fortunato, L.-C. Gerhardt, and S. Seeger, "A simple, one-step approach to durable and robust superhydrophobic textiles," *Advanced Functional Materials*, vol. 18, no. 22, pp. 3662–3669, 2008.
- [18] G. Momen and M. Farzaneh, "A ZnO-based nanocomposite coating with ultra-water repellent properties," *Applied Surface Science*, vol. 258, no. 15, pp. 5723–5728, 2012.
- [19] Z. Guo, F. Zhou, J. Hao, and W. Liu, "Stable biomimetic superhydrophobic engineering materials," *Journal of the American Chemical Society*, vol. 127, no. 45, pp. 15670–15671, 2005.
- [20] S. Wang, L. Feng, and L. Jiang, "One-step solution-immersion process for the fabrication of stable bionic superhydrophobic surfaces," *Advanced Materials*, vol. 18, no. 6, pp. 767–770, 2006.
- [21] T. T. Isimjan, T. Wang, and S. Rohani, "A novel method to prepare superhydrophobic, UV resistance and anti-corrosion steel surface," *Chemical Engineering Journal*, vol. 210, pp. 182–187, 2012.
- [22] D. W. Butler, C. T. H. Stoddart, and P. R. Stuart, *Aspects of Adhesion*, Edited by D. J. Alner, University of London Press, London, UK, 1971.
- [23] E. Darque and E. Felder, "Adhesion et adherence," in *Sciences et Techniques de l'Ingenieur*, CNRS, Paris, France, 2003.
- [24] I. Ramirez, E. A. Cherney, S. Jayaram, and M. Gauthier, "Nanofilled silicone dielectrics prepared with surfactant for outdoor insulation applications," *IEEE Transactions on Dielectrics and Electrical Insulation*, vol. 15, no. 1, pp. 228–235, 2008.



**Hindawi**

Submit your manuscripts at  
<http://www.hindawi.com>

